Cell Reports, Volume *36*

Supplemental information

Modulation of motor behavior by the mesencephalic locomotor region

Daniel Dautan, Adrienn Kovács, Tsogbadrakh Bayasgalan, Miguel A. Diaz-Acevedo, Balazs Pal, and Juan Mena-Segovia

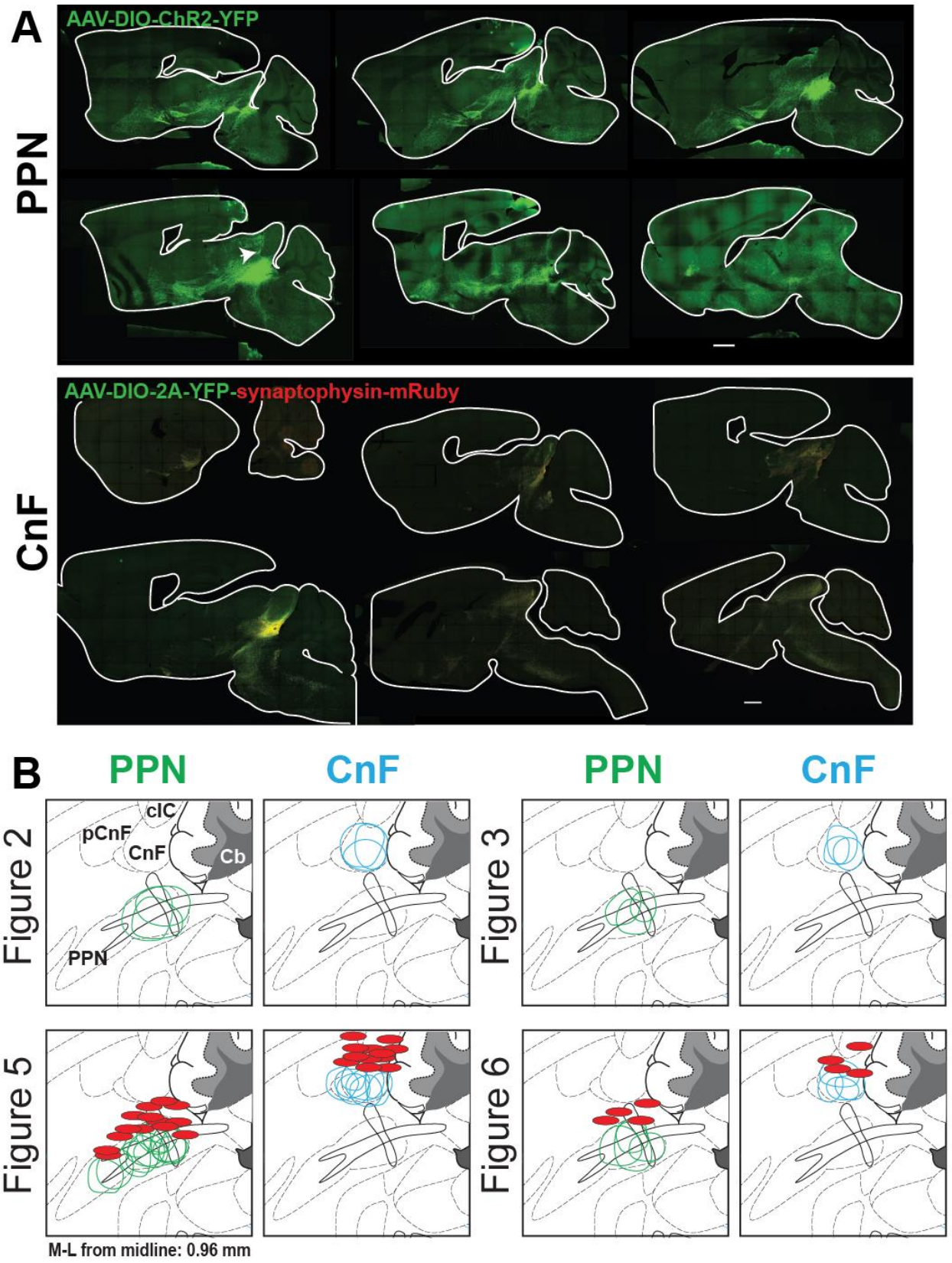

Supplementary Figure 1. Whole-brain images of MLR glutamatergic projections and histological analysis. Related to Figures 1, 2, 3, 5 and 6.

A, Fluorescent micrographs of PPN (top) and CnF (bottom) glutamatergic projections in the entire brain (6 representative sagittal sections) following transduction of VGLUT2-Cre mice. **B,** Virus spread (circles) and locations of the tip of the optic fibers (red circle) for PPN (green) and CnF (blue) groups. Data of transduction are represented as the maximum projection of the virus diffusion in the sagittal plane to allow better comparison. Scale bar: 1 mm.

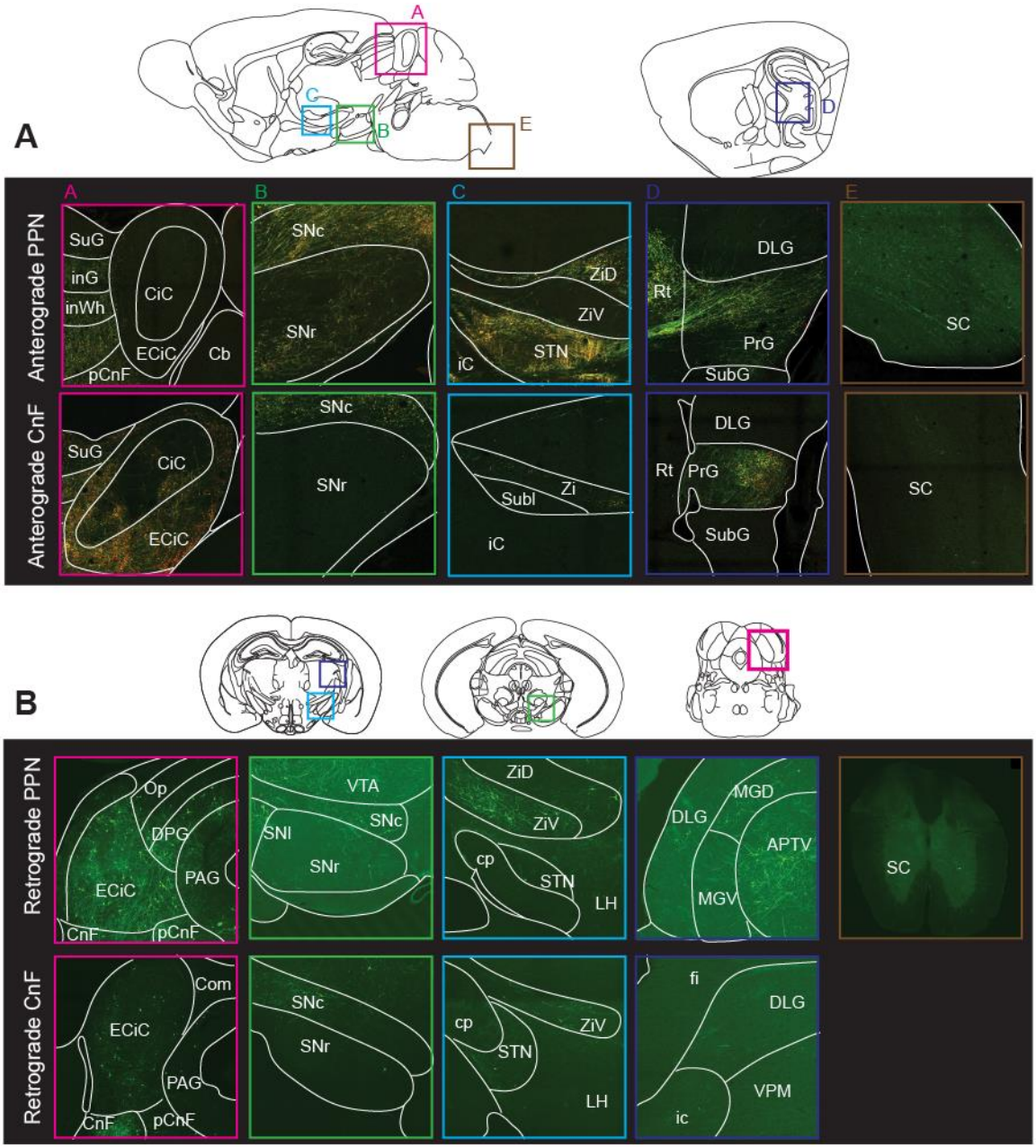

Supplementary Figure 2. Comparative examples of labeling of PPN and CnF afferents and efferents. **Related to Figures 2 and 3**.

Top, Representative examples of anterograde labeling following transduction of glutamatergic neurons in the PPN and CnF shown in the sagittal plane. Bottom, Representative examples of labeling of input neurons to the PPN and CnF glutamatergic neurons shown in the coronal plane. A, colliculus; B, SNr; C, STN and zona incerta; D, geniculate nucleus; E, spinal cord.

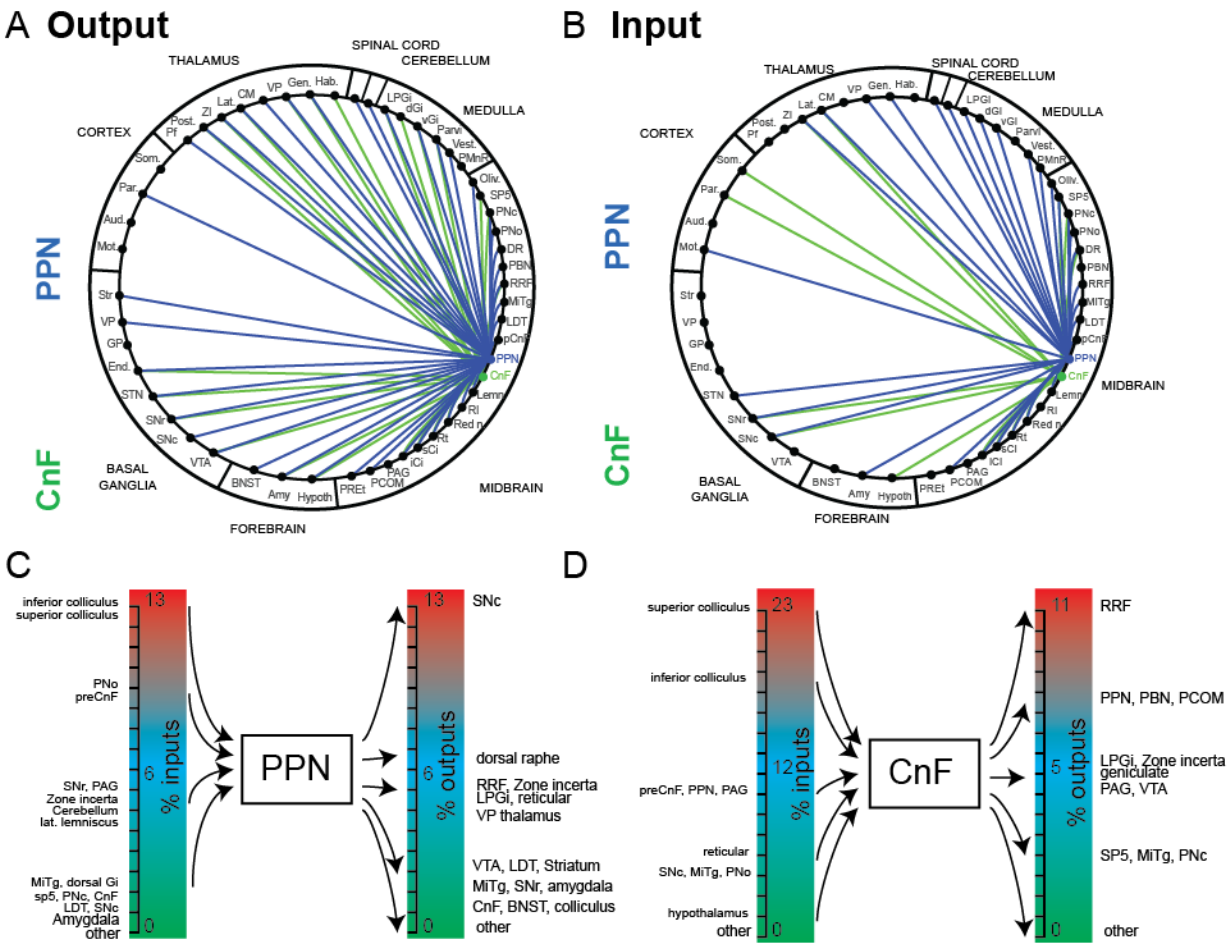

Supplementary Figure 3. Input/output relationship of PPN and CnF. Related to Figures 2 and 3.

A, Schematic summary of PPN (blue) and CnF glutamatergic (green) axonal distribution using relative synaptic density. **B**, Schematic summary of PPN (blue) and CnF glutamatergic (green) neuron inputs. **C-D,** Graphical representation of inputs and outputs of PPN and CnF glutamatergic neurons based on the data presented in Figures 2 and 3. Input arrows (left) are defined based on the normalized distribution of inputs neurons. Output arrows (right) are defined based on the normalized distribution of the synapses.

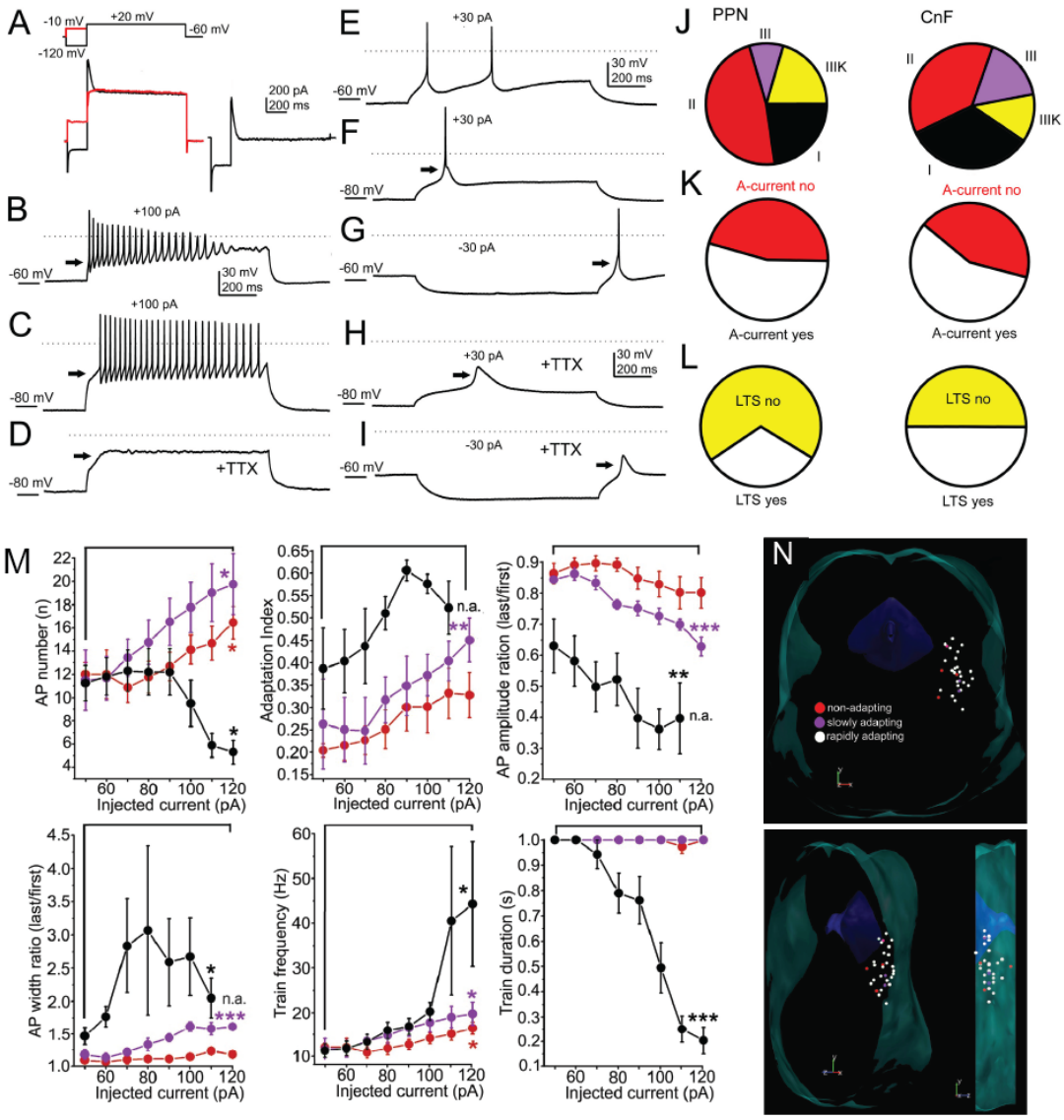

Supplementary Figure 4. Physiological properties of the PPN and CnF glutamatergic neurons and their spatial distribution. Related to Figure 4.

A, A-current was observed on most PPN and CnF glutamatergic neurons. Current traces elicited by +20 mV voltage step, preceded by -120 mV (black) and -10 mV (red) voltage steps (example shows PPN). The left current trace is the difference of the black and red current traces. **B-D,** Representative examples of the firing properties of PPN glutamatergic neurons. Trains of action potentials elicited by 100 pA depolarizing current injection from -59 mV (**B**), -87 mV (**C**) and -73 mV resting membrane potential (**D**, in the presence of TTX; the arrow indicates the lack of delay). **E-I,** Depolarization and action potential firing elicited by 30 pA depolarizing square current injection from -66 mV (**E**) and -83 mV (**F**) resting membrane potentials. Note the low threshold depolarizing spike (black arrow). (**G**) 30 pA hyperpolarizing current injection from -53 mV resting membrane potential revealed rebound spike and firing (black arrow). **H-I,** Low threshold spike and rebound depolarizing spike (respectively; arrow) in the presence of TTX. **J,** Distributions of functional neuronal types in the PPN and CnF. Group I neurons display low threshold depolarizing spikes but lack A-current (PPN: 22.7%, CnF 33.3%). Group II neurons display A-current (PPN: 47.7%, CnF 37.5%). Group III neurons display both (PPN: 9.1%, CnF 16.6%). Group IIIK lacks all (PPN: 20.5%, CnF 12.5%). **K,** Proportion of PPN and CnF neurons displaying A-current. **L,** Proportion of PPN and CnF neurons displaying low threshold spikes (LTS). **M**, Statistical summary of the number of action potentials elicited by 1-s depolarizing step, the adaptation index, the ratio of the amplitude of the last and first action potentials of the train, the ratio of the width of the last and first action potentials of the train, the frequency and the duration of the train in different functional subgroups (non-adapting, red; slowly adapting, purple; rapidly adapting, black). The significance was calculated between the first and last datapoints within each trace. * P<0.05, **P<0.01, ***P<0.001. **N,** Location of recorded neurons in a three-dimensional view in the coronal plane. All experiments have been replicated in at least 3 mice. All data are represented as mean ± SEM.

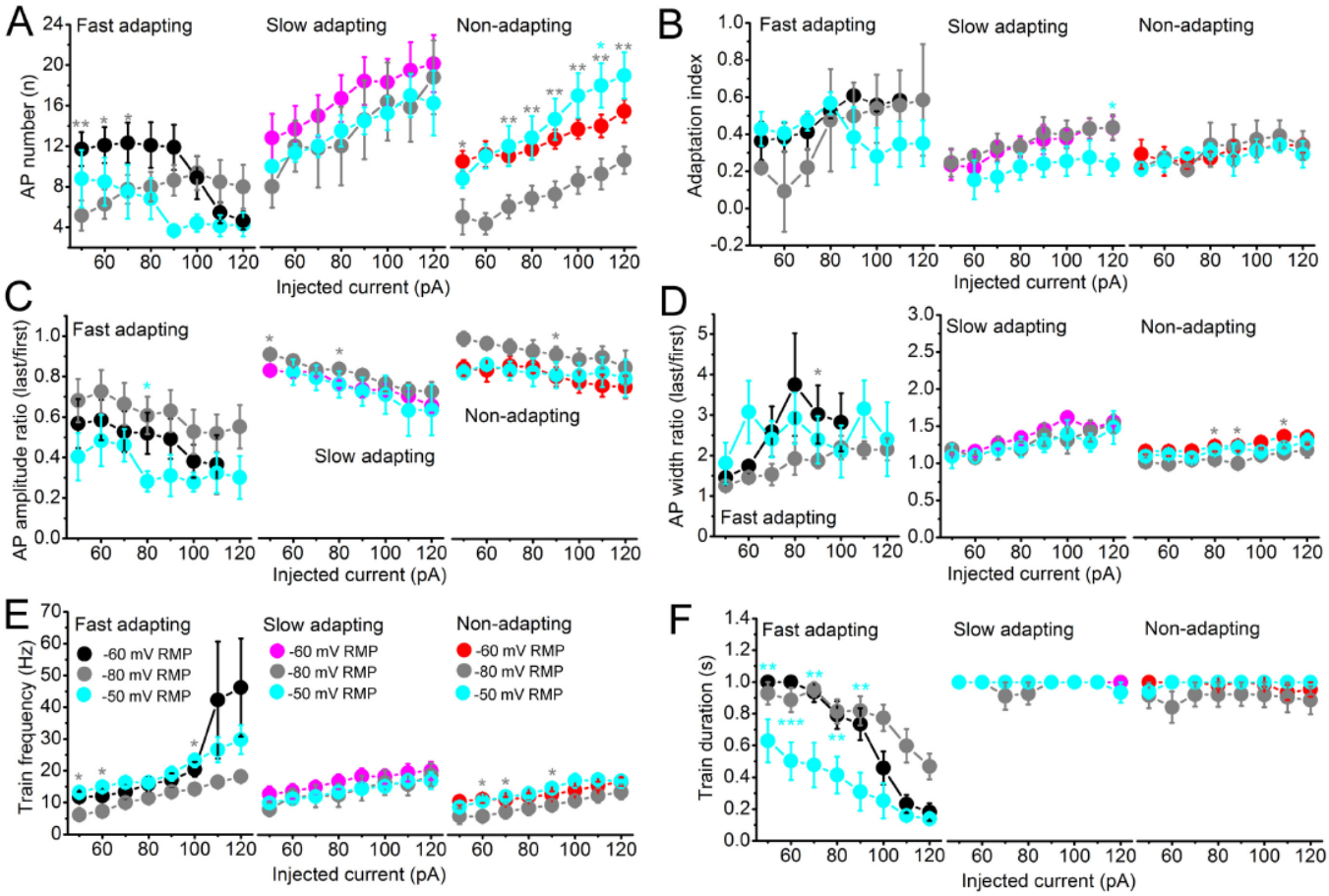

Supplementary Figure 5. Changes in electrophysiological parameters with different resting membrane potentials. Related to Figure 4.

A, Changes of average action potential firing frequency (AP number) elicited by square current injections. Black trace: fast adapting neuron with resting membrane potential set to -60 mV. Gray trace: neurons from the same group with resting membrane potential set to -80 mV. Blue trace: neurons from the same group with resting membrane potential set to -80 mV (see at panel **E**). Magenta traces: slow adapting neuron with resting membrane potential set to -60 mV. Red traces: non-adapting neuron with resting membrane potential set to -60 mV. Gray asterisks: significant difference between datasets recorded from -60 and -80 mV, blue asterisks: significant difference between datasets recorded from -50 and -60 mV. * $p < 0.05$; ** $p < 0.01$; *** $p < 0.001$. **B,** Changes of the adaptation index with the same color code as on panel **A** and **E**. **C,** Changes of the ratio of the first and last action potential amplitudes (AP amplitude ratio). **D,** Changes of the ratio of the first and last action potential width (AP width ratio). **E,** Changes of the action potential train frequency (i.e. parts of the voltage traces without action potentials are not included in calculation of the frequency). **F,** Changes of the action potential train duration.

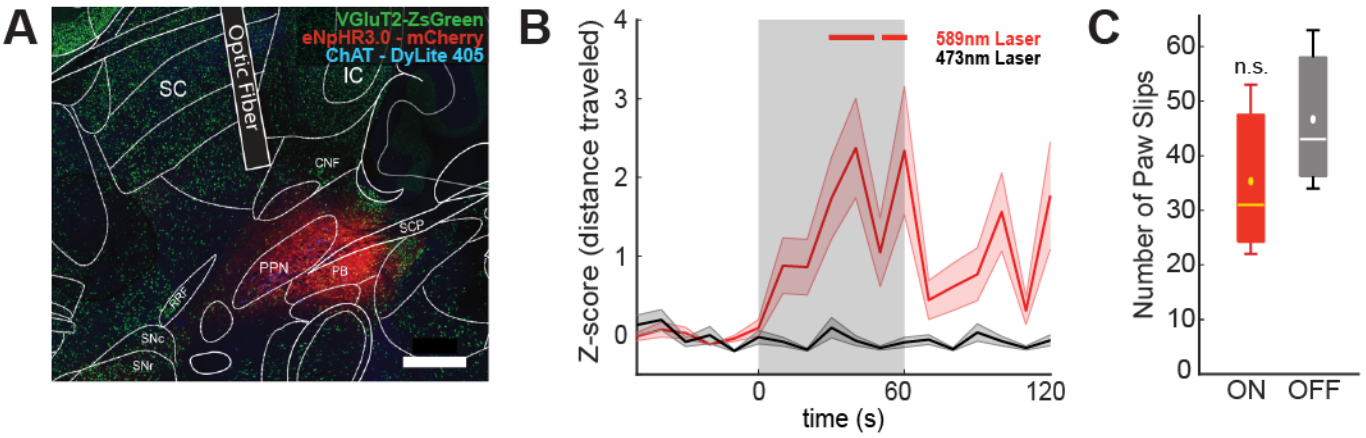

Supplementary Figure 6. Optogenetic inhibition of PPN glutamatergic neurons. Related to Figure 5.

A, Halorhodopsin (AAV5-Ef1a-DIO-eNpHR3.0-mCherry) was transduced into the PPN of VGluT2-Cre mice crossed with an Ai6 Reporter (n=3) and an optic fiber was chronically implanted approximately 200µm above the injection site. **B,** Normalized distance traveled (10s bin) during 1-min inhibition of PPN VGluT2+ neurons. t = 0 defined as onset of laser, shaded area represents time laser is on, control laser (473 nm) represented by black trace (two-way ANOVA, laser type x laserON: laser type effect $F_{(1,\ 608)}$=2.4, P=0.1217, stimulation effect $F_{(1,608)}$=0.15, P=0.7034, interaction effect $F_{(1,608)}$=2.1, P=0.1474. The line above represents statistically significant difference (mean Z-score > 1.96) of distance traveled relative to baseline (1 minute, 10s bins). **C,** The total number of foot slips during laser ON (red boxplot) compared to laser OFF (grey boxplot) on the elevated grid t(2)=-2.1634, P=0.1630. Scale bar: 500µm.

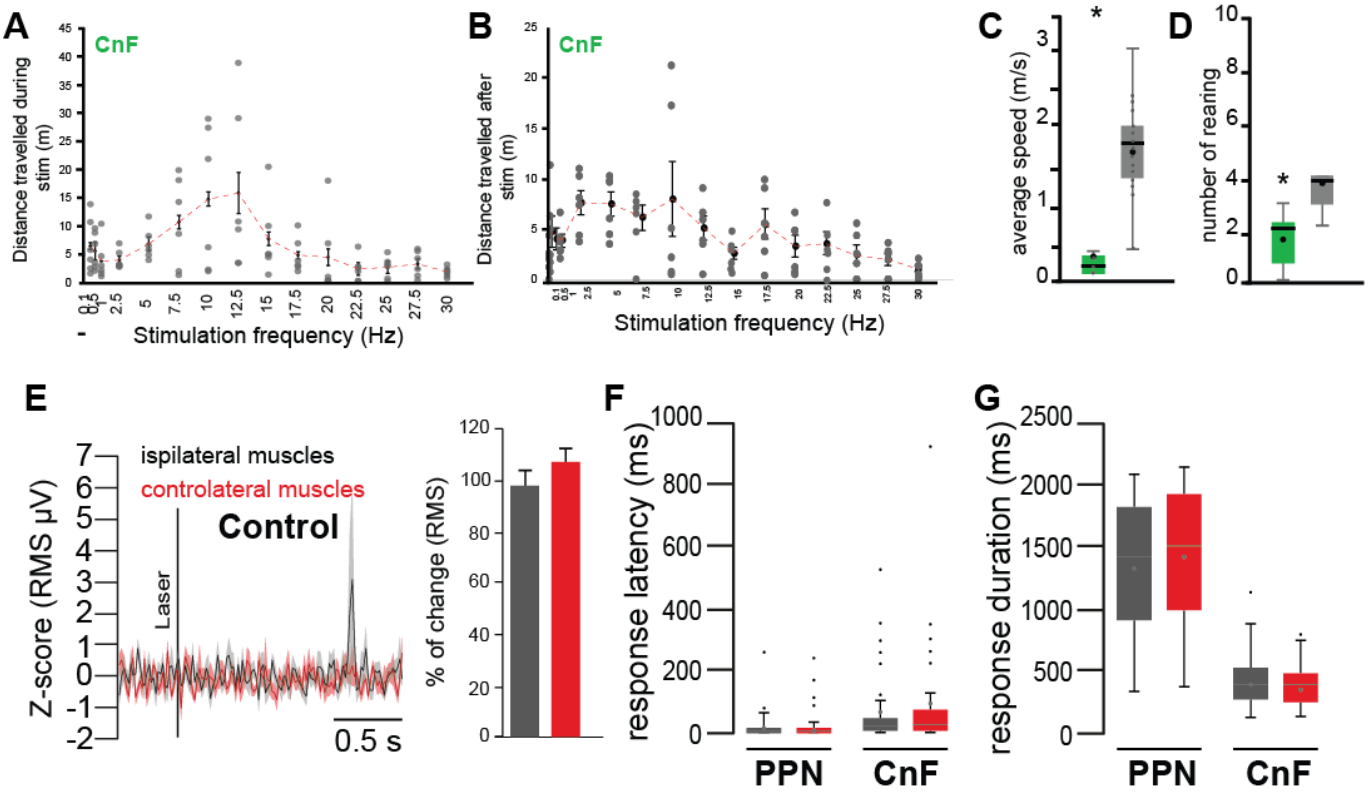

Supplementary Figure 7. Frequency-dependent modulation of locomotion in the CnF and complementary EMG experiments. Related to Figures 5, 6 and 7.

A-B, Distance traveled following optogenetic stimulation (1s ON/9s OFF) during and immediately after optogenetic stimulation of CnF glutamatergic neurons using a randomized stimulation protocol ranging from 0.1Hz to 30 Hz (mixed ANOVA; *during*: $F(14,89)=2.69$, $P=0.003$, trendline: $R^2 = 0.4774$, Max: 12.5, Posthoc Bonferroni $P=0.034$; *after*: $F(14,89)=1.24$, $P=0.2994$). Gray dots represent individual data points, black dots represents average values, vertical lines represent SEM, and the red line represents the best fitted trendline ($y=-0.0314x^2+0.7389x+4.9582$). **C,** Average speed of mice in the PPN (green) and control groups (gray) during the elevated grid walk test (t-test two tail: $t(28)=6.39$, $P=0.00001$). **D**, Total number of rearing events observed in the elevated grid walk test following stimulation of PPN glutamatergic neurons (green) and compared to control mice (gray; $t(15)=2.63$, $P=0.0095$). **E,** Z-score and % change in the RMS signal in the ipsilateral and contralateral biceps activity following stimulation of control animals (sham; $CTRL_{ipsi}$: 97.45±6.09%, $CTRL_{contra}$: 92.33±6.17, two-Way ANOVA stim x side: $F_{stim}(1,401)=0.18$, $P=0.67$, $F_{side}(1,401)=3.12$, $P=0.078$, $F_{interaction}(3,401)=18.30$, $P=0.093$). **F-G,** Response latency (two-way ANOVA target x side:$F_{target}(1,206)=14.24$, $P=0.0002$, $F_{side}(1,206)=0.14$, $P=0.71$, $F_{interaction}(1,206)=0.05$, $P=0.82$) and response duration (two-way ANOVA target x side:$F_{target}(1,212)=371.60$, $P=0.00001$, $F_{side}(1,212)=0.52$, $P=0.47$, $F_{interaction}(1,212)=1.39$, $P=0.23$) of the change in muscle activity following stimulation of PPN or CnF glutamatergic neurons (ipsilateral vs contralateral biceps).

Abbreviation	Structure
Amy	Amygdala
Aud	auditory cortex
BNST	Bed nucleus stria terminalis
CM	Centromedial thalamic n.
DR	Dorsal raphe
End	Endopeduncular nucleus
Gen	Geniculate nucleus
Gi	Gigantocellular nucleus
GP	Globus pallidus
Hab	Habenula
Hypoth	Hypothalamic nucleus
iCi	Inferior colliculus
Lat	Lateral
LDT	Laterodorsal tegmental nucleus
Lemn	Lemniscus nucleus
LPGi	Lateroposterior gigantocellular nucleus
M1	Primary motor cortex
MiTg	Microcellular tegmental nucleus
Mot	Motor cortex
n.	Nucleus
Oliv	Olivary nucleus
PAG	Periaqueductal gray nucleus
Parvi	Parvicellular nucleus
PCOM	Nucleus of the posterior commissure
Pf	Parafascicular thalamic nucleus
PMnR	Pontine mesencephalic nucleus
PNc	Pontine *caudalis*
Pno	Pontine *oralis*
Post.	posterior
preCnF	Precuneiform nucleus
RRF	Retrorubral field
Rt	Reticular nucleus
SC	Spinal cord
sCi	Superior colliculus
SNc	Substantia nigra *compacta*
SNl	Substantia nigra *lateralis*
SNr	Substantia nigra *reticulata*
Som	Somatosensory cortex
SP5	Spinal trigeminal nucleus
STN	Subthalamic nucleus
STR	Striatum
Vest	Vestibular nucleus
VP	Ventral pallidum
VTA	Ventral tegmental area
ZI	Zona incerta

Table S1. Abbreviations. Related to Figures 1-7.

Morphological parameters			
Parameter	**PPN**	**CnF**	**p**
Dendrite number	3.66 ± 0.33	5.11 ± 0.42	**0.007**
Node number	8.08 ± 1.51	15 ± 4.38	**0.05**
Ending number	11.58 ± 1.73	20 ± 4.56	**0.03**
Spine number	28.83 ± 8.7	32.11 ± 15.08	**0.42**
ChAT positivity (%)	3.4 ± 1.8 %	0 %	
n	77	41	
Functional parameters			
Parameter	**PPN**	**CnF**	**p**
A-current amplitude (pA)	395.13 ± 0.33	352.49 ± 52.15	0.32
M-current amplitude (pA; at -40 mV)	6.38 ± 1.76	11.5 ± 2.41	0.04
Persistent Na-current amplitude (pA)	26.61 ± 5.41	5.31 ± 3.11	0.005
Action potential delay at -60 mV resting membrane potential (ms)	31.27 ± 4.07	27.23 ± 7.95	0.311
Action potential delay at -80 mV resting membrane potential (ms)	61.39 ± 8.9 (p=0.0009 between delays at -60 and -80 mV)	44.67 ± 10.64 (p=0.09 between delays at -60 and -80 mV)	0.169
Low threshold depolarization amplitude (mV)	17.65 ± 3.09	12.07 ± 2.17	
Rebound depolarization amplitude (mV)	15.17 ± 2.99	13.09 ± 1.79	
Input resistance (MΩ)	818.93 ± 41.94	792.54 ± 77.9	0.21

Table S2. Morphological and functional parameters of PPN and CnF glutamatergic neurons. Related to Figure 4.

PPN (n = 44)	%	**CnF** (n = 24)	%
type I (LTS)	22.7	type I (LTS)	33.3
type II (first AP delay)	47.7	type II (first AP delay)	37.5
type III (LTS and first AP delay)	9.1	type III (LTS and first AP delay)	16.6
type IIIK (none of above)	20.5	type IIIK (none of above)	12.5

Table S3. Percentages of functional subtypes of PPN and CnF glutamatergic neurons. Related to Figure 4.